2015

CHARACTERIZATION OF SEISMICITY AT VOLCÁN BARÚ, PANAMA: MAY 2013 THROUGH APRIL 2014

Chet J. Hopp
Michigan Technological University

CHARACTERIZATION OF SEISMICITY AT VOLCÁN BARÚ, PANAMA: MAY 2013 THROUGH APRIL 2014

By

Chet J. Hopp

A THESIS

Submitted in partial fulfillment of the requirements for the degree of

MASTER OF SCIENCE

In Geophysics

MICHIGAN TECHNOLOGICAL UNIVERSITY

2015

This thesis has been approved in partial fulfillment of the requirements for the Degree of MASTER OF SCIENCE in Geophysics.

Department of Geological/Mining Engineering and Sciences

Thesis Advisor: *Gregory Waite*

Committee Member: *Rudiger Escobar Wolf*

Committee Member: *Petra Huentemeyer*

Department Chair/School Dean: *John Gierke*

Table of Contents

Preface

The work contained herein was undertaken by Chet Hopp in partial fulfillment of the requirements of a MS in Geophysics at Michigan Technological University. This included installation of seismometers, data collection, data analysis and interpretation, as well as preparation of this manuscript. Gregory Waite assisted with the planning and implementation of all phases of this project, specifically with data analysis and interpretation as well as with significant help in crafting this manuscript and the figures contained therein.

Acknowledgements

This project benefited, first and foremost, from the help of the people at OSOP Panama who donated time, expertise, advice, seismometers, server space, telemetry, office space and lodging for two years. Specific thanks go to Angel Rodriguez, Branden Christensen, Wilfried Strauch and Richard Boaz for serving as informal advisers and hosts and to Leandro Pérez for friendship, patience and wisdom beyond his years. Unlimited thanks go to the people of Peña Blanca, CNB, specifically my indigenous, Panamanian family Ofelina, Benito, Porfiria, Marcelino and all of the kids, for the courage to share their lives with a person they initially neither knew nor understood. My sanity as a Peace Corps volunteer would have been unsustainable if not for the friendship of my fellow PCV's, specifically Belligo, Chigo, Nido, Nicho, Bri and the entirety of G71. My sanity as a grad student would likewise have been unsustainable without the friendship of Ashley, Lauren, Marine, Fede, Bri and fellow RPCV's Nate, Jordan, Kyle, Tyler, Luke, Hans & Emily, Jarrod & Mariah, and Erica. Thanks are owed to my committee members Rudiger Escobar Wolf and Petra Huentemeyer for taking time out of their schedules and summer plans. Thanks go to my adviser Greg Waite for patience throughout, for making time for a trip to Panama to help get the project rolling and for allowing me the space and time to grow into this project and career.

Financial support for my time at Michigan Tech and throughout much of my Peace Corps service was provided by both NSF PIRE grant no. 0530109 and the United States Peace Corps. Thanks are owed to Eduardo Camacho of the University of Panama Institute of Geosciences for sharing freely of seismic data from stations at Banco and Potrerillos (BCO2 and PTAR3 in this study) as well as past data from Barú and unpublished reports.

Lastly, to those kind enough to host seismometers in their homes (and often a dirty gringo), the project would not have been possible without you: Finca Lerida (via the enthusiastic Doris Gonzales), Randy Piggott, Susan and Kerry Frank, Lloyd and Sandra Cripe, Dan and Kay Wade, Peter and Louise Mahoney and Branden Christensen.

Abstract

Volcán Barú, in the western province of Chiriquí, is Panama's youngest and most active volcano. Although Barú has experienced no historic eruptions there have been four eruptive episodes in the last 1600 years, the most recent occurring 400-500 years ago (Sherrod et al., 2007). In addition, there have been four reported earthquake swarms in the last 100 years. The most recent swarm occurred in May of 2006, prompting a USGS hazard assessment (Sherrod et al., 2007). In order to characterize local seismicity and provide a reference for future monitoring efforts, we established a seismic network that operated from May 2013 through April 2014. The network consisted of eight temporary single-component, short-period sensors loaned by OSOP Panama, and three permanent stations distributed over a 35 by 15 km area. During operation of the network a catalog of 91 local events were detected, located and then used to calculate a minimum 1-D velocity model for Barú. Of particular interest were a cluster of events west of the town of Boquete. A template matching detection technique was used to identify another 47 smaller magnitude events in the area of this cluster. Spectrograms for the largest events in the cluster show a broad band of frequencies up to ~20 Hz suggesting a predominantly tectonic source while eight focal mechanisms were calculated which suggest strike-slip and reverse faulting may be the predominant source processes. Further study is encouraged to better constrain the source processes and investigate how volcanic processes might affect local tectonics.[1]

[1]The material contained in this thesis is intended for submission to the *Journal of Volcanology and Geothermal Research.*

Introduction

Volcán Barú is located in Chiriquí Province, roughly 30 km East of the Costa Rica-Panama border and is Panama's highest point at 3,374 m. With populated areas to the east, west and south, including the city of David ~40 km to the southeast (pop. 82,000 (www.contraloria.gob.pa/inec/Publicaciones/) (Figure 1), Barú presents a significant hazard for more than 300,000 people (Universidad Tecnológica de Panamá, 1992) as well as to significant transportation, agriculture and tourism infrastructure. Given Barú's low level of historic eruptive activity, local earthquakes may present the most immediate threat to lives and property. Residents of the small towns on the flanks of Barú, specifically in the area surrounding Boquete, feel and hear earthquakes on a monthly basis. These events are often described as sounding like 'trains', 'thunderstorms' or 'roars' followed by a strong 'blow' or 'smack' to the house. Some of these events likely originate at fracture zones off the southern coast of western Panama. However, significant seismic activity also originates from the area surrounding the volcano (Cowan et al., 1996; Camacho, 2009; Toral and Ho, 2006). The most notable recent activity was an earthquake

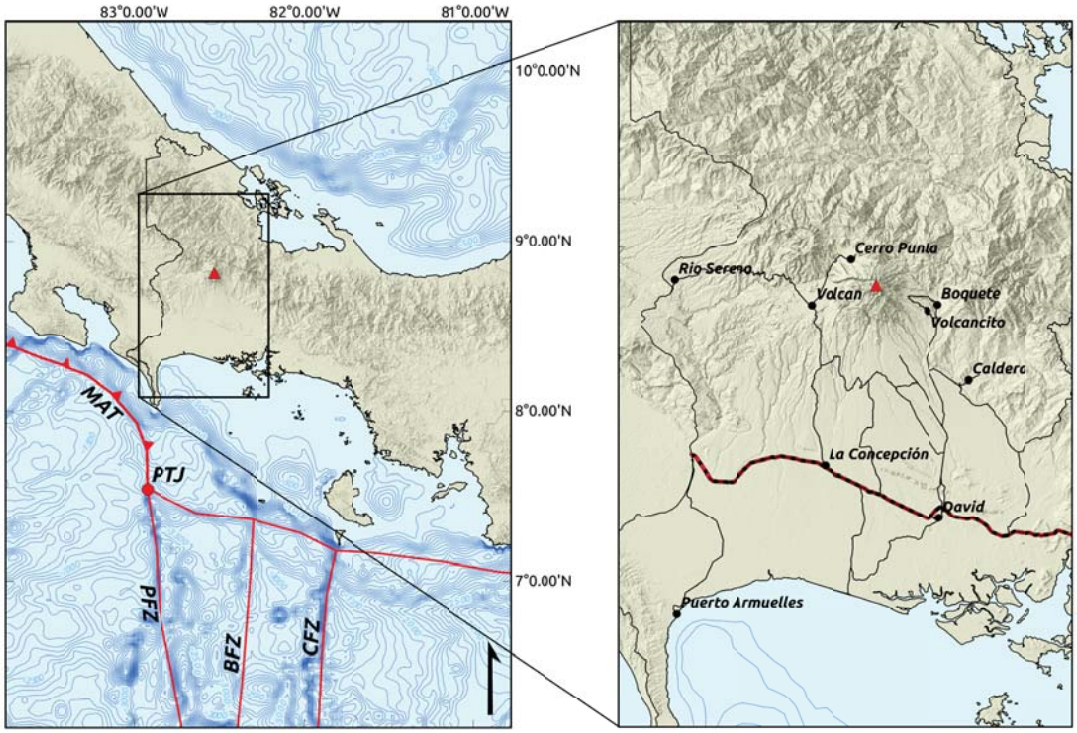

Figure 1: Map on the left shows tectonic features of W. Panama and S. Costa Rica (adapted from Morell et al. 2013). MAT- Middle America Trench; PTJ- Panama triple junction; PFZ- Panama fracture zone; BFZ- Balboa fracture zone; CFZ- Coiba fracture zone; Barú is marked by red triangle; 100 m bathymetric contours created from ETOPO1. Inset map shows key cities/towns near Barú. The extent of the Panamerican highway to the Panama-Costa Rica border is shown as a red-black dashed line; other major roads shown as black lines. Hillshade created from NASA SRTM v3 imagery, road layers created from OpenStreetMap via the QGIS software package.

swarm occurring in May of 2006, which included events up to M_L 4.7 and prompted a USGS hazard assessment of Barú (Toral and Ho, 2006; Sherrod et al., 2007). Partially as a result of this swarm, a seismic monitoring network was installed on Barú from June 2006 through August 2008 (Camacho et al., 2008).

The objective of this study was to assess the contemporary nature of seismicity around Barú with a temporary seismic network. We present a new dataset consisting of earthquakes occurring between early May 2012 and the end of April 2013 in the area surrounding the volcano. A 1-D velocity model for Barú was computed using these events via the joint velocity model-hypocenter inversion program *Velest* (Kissling et al., 1994). The resulting relocated hypocenters revealed a small cluster of events beneath the volcano's eastern flank which was further investigated. A template matching technique was used to detect additional, smaller magnitude events from this cluster which were then relocated using the double-difference location program *HypoDD* (Waldhauser and Ellsworth, 2000). A spectrogram and focal mechanisms from this earthquake cluster are presented as well as signal duration magnitudes which were calculated for most of the catalog. Finally, the characteristics of local seismicity across the dataset are discussed.

Background

Geologic context

Barú is Panama's youngest volcanic center and marks the southern end of the active Central American Volcanic Arc (CAVA) (Carr et al., 2003; Hidalgo and Rooney, 2010). However, the approximately 175 km gap between it and the volcanoes of central Costa Rica suggests Barú, and nearby Tisingal, represent a volcanic zone distinct from the rest of the CAVA (Carr et al., 2003, Hidalgo and Rooney, 2014). This distinction is supported by the presence of adakitic lavas at several of Panama's volcanic centers (Carr et al., 2003, de Boer et al., 1991, Defant et al., 1992, Hidalgo and Rooney, 2010, 2014); rocks not found elsewhere in the CAVA but which represent the bulk of Barú's edifice (Hidalgo and Rooney, 2014). Adakite geochemistry is often associated with melting of the downgoing slab (Defant et al., 1991, 1992, Carr et al., 2003, Wegner et al., 2011). However, Hidalgo and Rooney (2014) suggest that Barú is much too voluminous to have been derived from melting of the down-going Nazca plate. They suggest that it is instead more similar to typical arc volcanoes; the adakites having perhaps evolved via fractionation processes at the base of the crust (Hidalgo and Rooney, 2014).

Tectonic Setting

Western Panama and southern Costa Rica are zones of significant seismicity (Muñoz, 1988a; Camacho, 2009). Earthquakes originate, predominantly, from right-lateral transverse faults dividing the subducting Cocos and Nazca plates offshore of the Panama-Costa Rica border (Adamek et al., 1988; Muñoz, 1988a,1988b). From west to east these fracture zones are referred to as the Panama, Balboa and Coiba Fracture Zones

(PFZ, BFZ, CFZ) (Morell et. al., 2013) with slip rates on the most active of these, the PFZ, being greater than 50 mm/yr (Cowan et al., 1998). Slip on the BFZ is an order of magnitude less than on the PFZ while the CFZ is thought to be extinct (Morell et. al., 2013). The intersection of the PFZ with the overriding Caribbean Plate at the Middle America Trench defines the Panama Triple Junction (PTJ) and also represents the end of trench-normal subduction of the Cocos plate beneath the Panama microplate in Costa Rica and the beginning of oblique subduction of the Nazca plate below western Panama (Morell et al., 2013) (Figure 1). Seismicity along the Panamá-Costa Rica border, from Punta Burrica northward reflects an interaction between the subducted PFZ and the Panama microplate, with normal and thrust faulting mechanisms observed (Muñoz, 1988a,1988b). Other sources of regional seismicity include a series of imbricate thrust faults associated with the subduction of the Cocos Ridge offboard southern Costa Rica (known as the Fila Costeña) (Morell et. al., 2013) as well as the North Panama Deformed Belt (NPDB), a zone of seismicity off the coast of northern Panama probably associated with active subduction of the Caribbean plate below the Panama microplate (Muñoz, 1988b; Camacho, 1993, 2010).

Barú's edifice encompasses an area of some 280 km^2 (Sherrod et al., 2007). Estimates of the total volume of erupted material range from 250 km^3 (Sherrod et al., 2007) to 450 km^3 (Hidalgo and Rooney, 2014). The majority of this erupted over a span of less than 213 kyr (Hidalgo and Rooney, 2014) although volcanism in the area began as early as the Tertiary (Wegner et al., 2011). The volume of the current edifice is less than these estimates of erupted volume suggest due to two large volcanic debris avalanches, which together cover an area greater than 1000 km^2 (Herrick, 2013; Morell et al., 2013). The deposits extend from the western flank of the volcano to the Pacific ocean some 60 km distant (Morell et al., 2013, Herrick, 2013). Bathymetric maps suggest that these deposits extend past the modern coastline into Charco Azul Bay (Morell et al., 2013) and are the largest such deposits known in Central America (Sherrod et al., 2007). The volcano itself bears a distinctive, westward-facing, horseshoe-shaped scar often associated with large sector collapse events (Herrick, 2013; Sherrod et al., 2007). Within this collapse feature, a newer lava dome feature has emerged from which the volcano's recent eruptions likely originated (Sherrod et al., 2007). Age dating of charcoals within recent volcanic deposits at Barú was undertaken as part of a USGS hazard assessment in 2007 (Sherrod et al., 2007). The study concluded that there have been a minimum of 4 eruptive episodes in the last 1,600 years (Sherrod et al., 2007) which were characterized by “prolonged dome growth, explosive eruptions, and the spalling of numerous block-and-ash flows.” (Sherrod et al., 2007, pg. 15). The most recent eruption, as indicated by C^{14} dating of charcoal within volcanic deposits as well as stratigraphic observation, occurred between roughly 400 and 550 years B. P. (Sherrod et al., 2007, Hidalgo and Rooney, 2014). This suggests that Barú, regardless of it current period of quiescence, is still an active volcano.

Local seismicity

The history of local seismicity at Barú is largely unknown (Sherrod et al., 2007), however mostly anecdotal evidence suggests that local earthquake swarms occurred in 1930, 1963, and 1985 (Sherrod et al., 2007). From 4 to 10 May, 2006, a swarm of more than 20 earthquakes was recorded in the area of Boquete (Toral and Ho, 2006; Camacho 2009, Sherrod et al., 2007). These events were recorded either by the Panamanian Red Nacional de Movimientos Fuertes (National Strong Motion Network) or on a temporary network used by the Universidad Tecnológica de Panamá (UTP) which was installed on 8 May to investigate the swarm (Toral and Ho, 2006) (see Appendix A: Figure 10). The seven largest events of the swarm, ranging from M_L 4.0 to 4.7, were reported from 4 to 6 May (Toral and Ho, 2006). Ten additional events of M_L 2.2 to 3.1 were reported from 8 to 10 May (Toral and Ho, 2006). Hypocentral depths for the entire swarm ranged from 1.2 to 10 km (Toral and Ho, 2006). The 2006 swarm prompted the USGS hazard assessment mentioned earlier as well as efforts to more comprehensively monitor Volcán Barú's activity; the need for which had been recognized since at least 1992 when the UTP compiled an extensive risk assessment for the volcano (UTP, 1992).

A permanent network (Appendix A: Figure 11) was established by the University of Panama in conjunction with the Panamanian government (Camacho et al., 2008) and the private company OSOP, based in the town of Volcán on Barú's western flank. This network was in place from June 2006 until August 2008 (Camacho et al., 2008) but was dismantled in the following years. Currently there are permanent stations at Banco (BCO2), Potrerillos (PTAR3) and near Barriles (BRU2) at the locations shown in Figure 2.

Mapping of local faults is limited. Restrepo (1987, pp. 48-50, Fig. 22) suggests that regional NW-SE striking normal faults developed prior to Pliestocene volcanism at neighboring Tisingal but that changes in regional stresses later developed sets of SW-NE and W-E striking faults. These younger features truncate Tisingal and are possibly related to the shift of the volcanic center from Tisingal to Barú (Restrepo, 1987). Sherrod and others (2007, pp. 11) map a set of faults striking WNW-ESE across the northern flank of the volcano which agree with the idea of pre-volcanism normal faulting. Multiple sources (Camacho et al., 2008; Camacho, 2009; Toral and Ho, 2006) also reference sets of smaller scale faults striking both NW-SE and NE-SW in agreement with a later change in the regional stress regime. Published focal mechanisms indicate left lateral strike-slip movement, reverse faulting or a combination of both on these faults (Camacho, 2009; Cowan et al., 1996; Toral and Ho, 2006).

Methodology

Network

This study made use of equipment designed, manufactured and donated by OSOP. Eight of the seismometers were short-period, vertical-component instruments called Dariens, each containing a single 4.5 Hz geophone with a corner frequency electronically

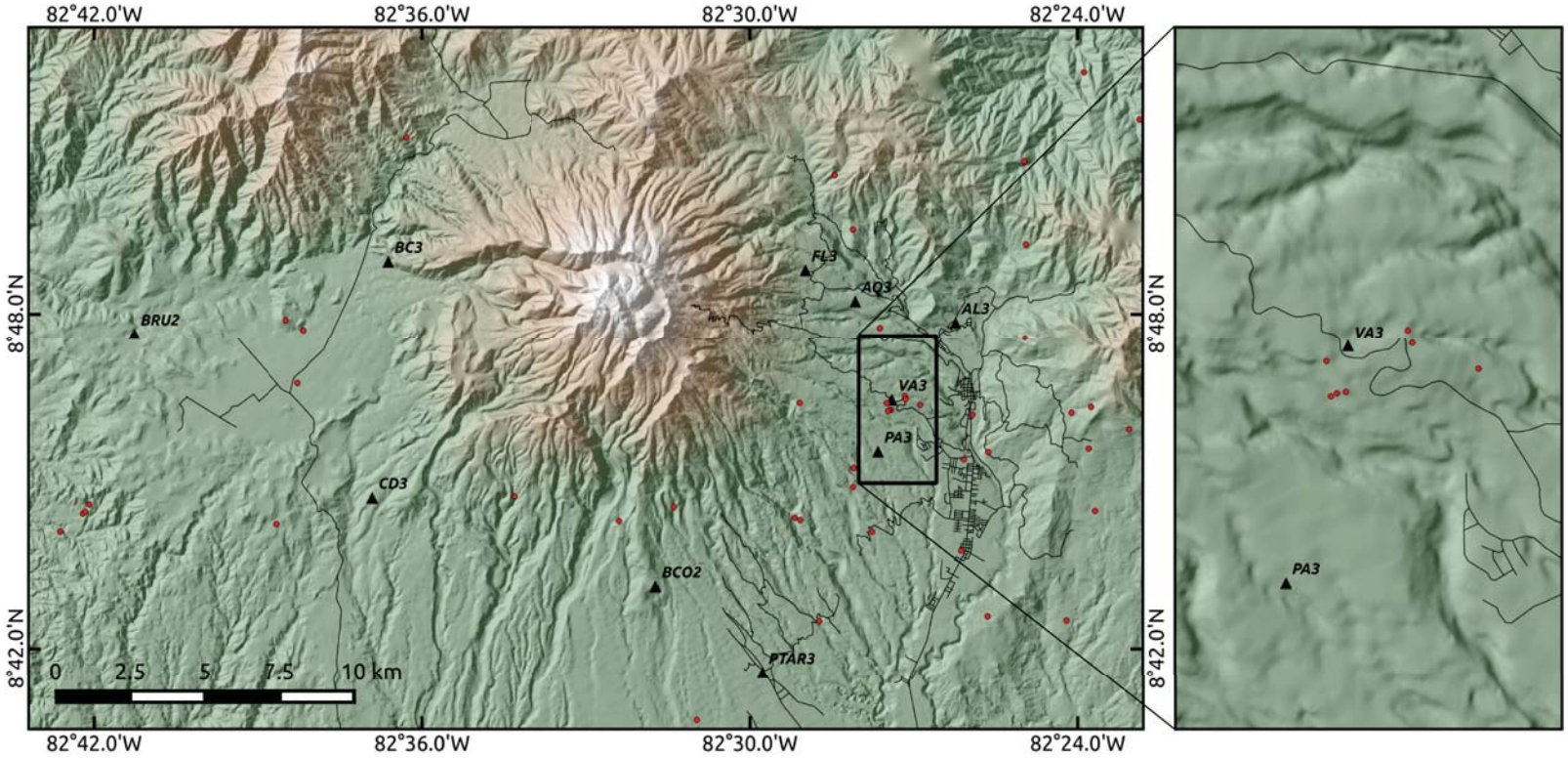

Figure 2: Map shows the locations of the seismometers used in this study (black triangles). Also shown are Velest *relocations of earthquakes for the period of May 2013 through April 2014. Note that some of the 91 events in the catalog were located outside of the map area and are not shown. The inset map provides detail on the 'Volcancito cluster' of events referred to throughout this paper.*

extended to 2 seconds as well as two horizontal accelerometers. One station (BCO2) was an OSOP designed, three-component Sixaola which uses the same geophones as the Dariens. Timing for the Darien is done via NTP with an estimated maximum timing uncertainty of +/- 40 ms at a sample rate of 50 Hz (Timing, n.d.). The Sixaola has the added capability of using an external GPS and both instruments contain on-board 24-bit digitizers. One permanent trillium compact broadband instrument (BRU2) was made available to us for the purposes of this study. The BRU2 data is also available through the IRIS DMC.

For this study we installed 7 Dariens around the volcano, all roughly 5-7 km from the summit. The University of Panama Facultad de Geociencias made available data from one preexisting Darien (PTAR3) and one Sixaola (BCO2) which was installed by OSOP during the course of this study. The aforementioned broadband instrument (BRU2) completed the ten station network shown in Figure 2.

Given that the instruments required power-over-Ethernet, stations could only be sited in houses and businesses with internet connection. This provided good security but led to high levels of anthropogenic noise. Instruments were sited in a roughly circular geometry around the volcano, however, given areas of low population density and lack of internet connection, a notable gap exists to the north of Barú. Considering higher levels of historical seismicity on the volcano's eastern flank (Camacho et. al., 2008; Toral and Ho, 2006), priority was given to installing instruments in the area around Boquete.

Data Analysis

1. Initial detection and location

Data acquisition and archiving was handled in real-time via *SeisComP3* software at OSOP in Volcán and saved as day-long miniSEED files. Potential problems with each station were remotely monitored throughout this study using USGS *SWARM* software (http://volcanoes.usgs.gov/software/swarm).

Initial earthquake detection and phase picking was done using the BRTT *ANTELOPE* software package (www.brtt.com/software). Detections were obtained using a Short Term Average/Long Term Average (STA/LTA) detection algorithm. Data were bandpass filtered from 2 to 10 Hz with STA/LTA windows of 1 and 10 seconds respectively. All phase picks were reviewed by hand before relocating. All events located within two degrees of at least two stations were defined as 'local' and used in the analysis described below. All other events were defined as 'regional/teleseismic', likely originating from the PFZ or near the Costa Rican border and ignored for the purposes of this study.

2. Velocity model and relocation

Local events were then used to obtain a 1-D velocity model using the joint hypocenter-velocity model program *Velest* (Kissling et al., 1994). Given the non-linear nature of the hypocenter-velocity model problem, multiple runs of *Velest*, each with a

unique starting velocity model, are necessary to identify the best fit solution (Kissling et al., 1994). The model with the lowest root-mean-square (RMS) misfit must be approached from various directions, utilizing starting models with both high and low velocities as well as with varying layer thickness (Kissling et al., 1994). In this way confidence is built that the final solution represents the overall minimum RMS misfit for the entire solution space and not solely a local minimum. Thirty *Velest* runs were used to explore the solution space and determine the most likely 1-D models for Volcán Barú (Figure 3D) as well as station corrections across the network (Figure 3A). Once these best-fit velocity models were found, the station and velocity parameters were fully damped, allowing *Velest* to solve for only the hypocenters of each of the 91 events in the dataset.

3. Template matching technique

Relocation of the events with *Velest* revealed a cluster of seven earthquakes west of the town of Boquete in an area known as Volcancito (see inset, Figure 2). To further investigate these events, a template matching technique similar to that used by Shelly and others (2007) was used. The waveforms recorded for each of the seven events (hereafter referred to as 'templates') were cross-correlated with the entire dataset. Correlation coefficients were calculated between template events and catalog data at each station at a sample rate of 25 Hz. These correlation coefficients were then averaged across the network, yielding a 'template correlation' for each template event at a given time. The averaging step differed from the technique used by Shelly and others (2007) who summed correlation values for every channel. However, for this dataset, a summed correlation proved extremely sensitive to times when parts of the network were not operating. Creating an average 'template correlation' value was less dependent on the number of stations in operation. A threshold template correlation value was then tuned to accommodate the high levels of anthropogenic noise across the network which caused much higher correlations during daytime hours than at night. This diurnal effect was worsened when the number of stations in operation was low, leading to high numbers of false detections. To account for this, two threshold values were used. A threshold correlation value of 0.30 was used when fewer than 8 channels were in operation whereas a threshold of 0.21 was used when 8 or more channels were in operation. When these thresholds were exceeded a detection was recorded.

Events which caused a detection had waveforms which were very similar to the template events and, therefore, could be assumed to have occurred at roughly the same locations. However, while highly similar, these waveforms were not identical. Differences between the detected waveform and the template waveform at a given station must be due to 1) timing errors or 2) differences in earthquake location and, therefore, also the path of the ray. It should be noted that large maximum NTP timing errors (+/-40 ms) may have lead to large errors in arrival time picking.

If the arrival times of a detected event were different than the arrival times of the template event they needed to be updated in order to calculate an accurate location. To account for this, once a detection was recorded, the template waveforms were allowed to

shift up to one second before and one second after the initial detection. For each station, the cross-correlation was re-run over this two second window. If a higher correlation value was found than the original correlation at the time of detection the arrival time was updated. Travel times were then output for use with the double-difference relocation program *HypoDD*.

4. Double difference relocation

In order to locate the events detected by the template matching technique described above, the 1-D velocity model calculated using *Velest* was paired with the double-difference earthquake location program *HypoDD* (Waldhauser and Ellsworth, 2000). *HypoDD* is capable of using both catalog arrival time differences and delay times derived from cross correlation of event waveforms. However, for this study, only the catalog travel times from the template matching script were used. Given the distance of stations BC3 and CD3 from the hypocenters, P-wave arrivals for the smaller magnitude events were poorly recorded at these locations. These picks were down-weighted for the double-difference relocation. Starting locations in *HypoDD* for each newly detected earthquake were assigned the location of the template event with the highest average correlation value at the time of detection. Weights for each arrival pick were set as the square of the template correlation at that station.

5. Focal mechanisms and signal duration magnitudes

Eight focal mechanisms were calculated for five of the template events as well as three other events detected with the STA/LTA algorithm using program *FPFIT* (Reasenberg and Oppenheimer, 1985) (Figure 7). Finally, signal duration magnitudes (M_d) following the technique used by Lee and others (1972) were calculated for 36 events from the STA/LTA detection catalog, specifically those events located within or close to the network, as well as all 47 events detected using the template matching technique.

Results and Discussion

Initial detection and location

Initial detection using the STA/LTA algorithm produced 808 detections most of which were located near either the Panama-Costa Rica border or offshore near the PFZ. Of the 808 initial events, 91 events were located within two degrees of at least two stations in the network, and therefore defined as 'local' for the purposes of this study. Initial hypocenters for these 91 events were well distributed but the majority were located to the east of the summit of Barú. This is consistent with reports of local seismicity (Astigarrabia, 2003; Camacho et al., 2008; Camacho, 2009; Toral and Ho, 2006) and consistent with the hypocenters of the May 2006 swarm (Toral and Ho, 2006) (Appendix A: Figures. 10, 11). Events located beyond the circumference of the network have larger azimuthal gaps and, as a result, larger absolute location errors.

Velocity model and relocation

Figure 2 shows the hypocenters of the 91 local events after the *Velest* relocation. Hypocenters are well distributed with a greater concentration of events on the eastern flank of Barú around the town of Boquete, again consistent with previous reports (Camacho, 2009; Toral and Ho, 2006). These relocations appear to cluster together more than the initial *Antelope* locations and the concentration of events on the east side of Barú is more pronounced. However, seismicity remains well distributed around the volcano. Of particular interest following the relocation was a small cluster of 7 events west of Boquete in an area called Volcancito (see inset, Figure 1). This small cluster was the focus of the following analysis.

Figure 3D shows the three best fitting 1-D P-wave velocity models obtained for Volcán Barú after 30 *Velest* inversions, each with an RMS less than 0.092. Figures 3A, 3B and 3C show 7 selected earthquakes and how their hypocenters vary from one velocity model to the next. The final velocity model used for this study, with an RMS of 0.0908, is shown in red, however it is important to note that all three 1-D models shown have RMS values within 0.001. Choosing between them without further knowledge of the subsurface at Barú or a larger dataset is largely arbitrary. Furthermore, variation in event hypocenters between the three 1-D models is not enough to significantly alter interpretations of local seismicity (see Figures 3A, 3B, 3C). Absolute location errors across the entire dataset range from 0.2 to 4.9 km and are largely dependent upon the location of the event. Events located outside the network have larger location errors than events located within or very near the network. The seven 'template' events in the Volcancito cluster examined throughout this analysis had absolute location errors of between 3.2 and 4.3 km. However, these events remained clustered regardless of which 1-D model was used. This suggests that, although the absolute location of the cluster is subject to some speculation, the existence of the cluster is not.

Station corrections across the network ranged from -0.14 to +0.14 seconds (Figure 3A). Stations to the west of the volcano show negative corrections (fast paths) while those to the east show the opposite (slow paths).

Velocity model layers between 4 and 18 km depth are particularly well constrained as they contain the majority of the hypocenters and many of the rays passing through them are sub-horizontal in nature. The velocities of these layers converged to between 5.75 and 6.50 km/sec regardless of the starting velocity model. Less well constrained are the shallowest (-3 km to 2 km depth) and deepest (>34 km depth) layers. Because of this, the two deepest layers (34-43 km and >43 km depth) were fixed to iasp91 velocities. In the case of the shallowest layers, the lack of model constraint is due to the vertical nature of the raypaths. This means that raypath travel times contain little information about P-wave velocity in the shallowest layers because the distance traveled through these layers is small when compared to the total length of the raypath.

Template matching technique

An example of template waveforms and the corresponding spectrogram used for the template matching are shown in Figure 4. Shown is the average spectrogram across

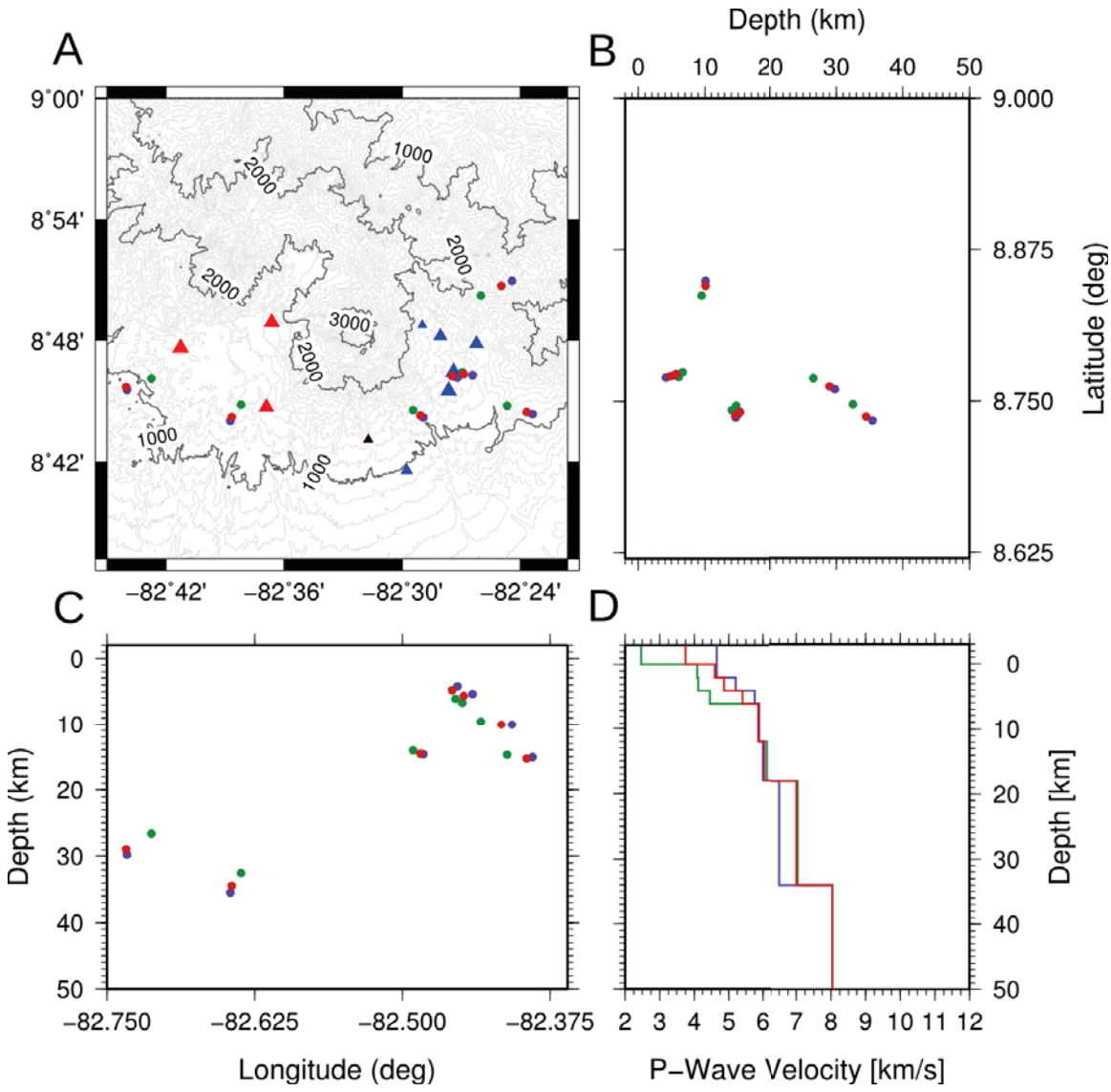

Figure 3: 7 Velest *hypocenters and their variation across 3 different velocity models. Locations are color coded to correspond to the 1-D velocity models with which they were calculated (Fig. 3D). The models shown had RMS values of less than 0.092 and represent the 3 best fitting solutions for this dataset. Stations are represented as triangles in Fig. 3A sized by P-wave station corrections. Red stations signify negative station corrections, blue signify positive. The reference station (BCO2) is colored black. Contours in Fig. 3A are in meters. Figs. 3B and 3C show depth cross-sections with latitude and longitude, respectively.*

all channels for the first event on October 11, 2013. Given the large frequency band (to beyond 20 Hz) and impulsive arrival, these events are likely products of predominantly tectonic processes. This is in agreement with the results presented by Camacho (et al., 2008; 2009) and Toral and Ho (2006). However, the role volcanic processes may play in controlling earthquake activity locally cannot be discounted. Manual review of the template matching detections allowed us to identify a number of false detections which

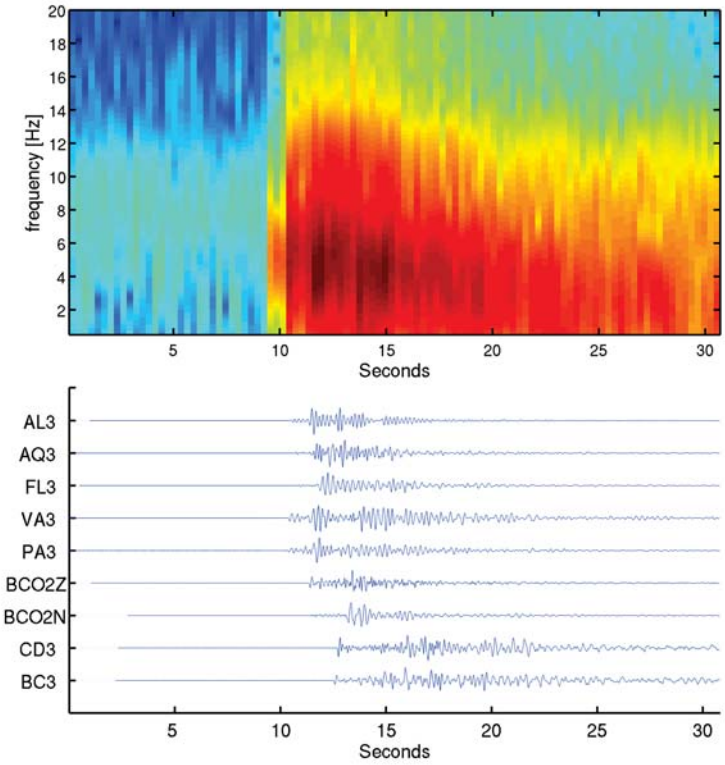

Figure 4: Spectrogram and waveforms for the largest magnitude event on October 11, 2013. Spectrogram depicts spectra averaged over all vertical channels in the network.

were due to high noise levels on certain stations. After exclusion of the template events themselves, 47 additional events were detected using the technique. Of these 47 events, 20 occurred during two bursts of activity on October 11, 2013 and December 10, 2013 of 14 and 6 earthquakes respectively. Four of the seven template events occurred on these two days; two on October 11 and two on December 10. These four templates account for the majority of the detections using this technique which suggests that these events reflect the most common source processes throughout the year. An example detection from one of these events is shown in Figure 5 with the corresponding average correlation value plot.

Double difference relocation

The 55 events detected by the template matching technique (including the seven template events) were relocated using *HypoDD* and are shown in Figure 6. Individual earthquakes are represented in the plot by red circles. These hypocenters define a cluster between roughly five and six kilometers depth located approximately three kilometers west of Boquete; an area known locally as Volcancito. The cluster defines a roughly NW-

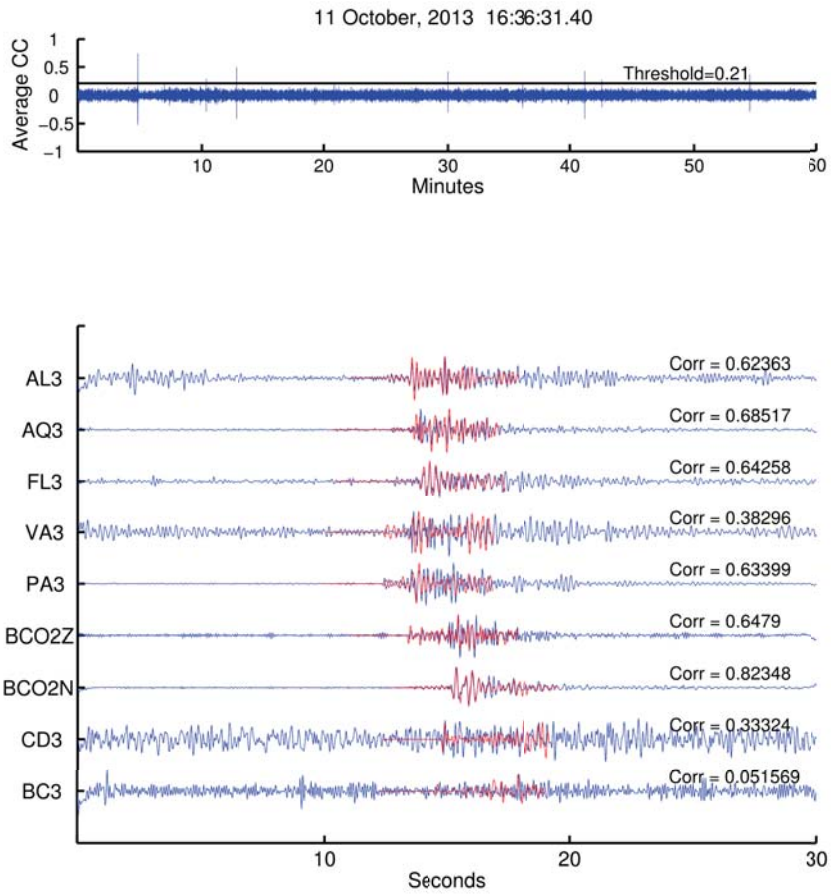

Figure 5: Example matched filter detection on October 11, 2013. Template event shown in red overlaid on actual data in blue. Correlation values for each station are shown above each trace. Upper plot depicts the averaged correlation value for the template event across all stations beginning 30 minutes before detection of the event.

SE striking trend. It is possible that these events are related to a set of NW-SE striking faults indicated in Toral and Ho (2006, pp. 15, Fig. 20) as well as Camacho (2009).

Focal mechanisms and signal duration magnitudes

Figure 7 shows eight lower hemisphere fault-plane solutions accompanied by first arrival waveforms for each station. These events were some of the largest magnitude events in the dataset and were, therefore, best recorded on all stations, allowing for the most robust focal mechanism solutions. The best fit solutions suggests strike-slip and reverse faulting may be an important mechanisms in the cluster as well as on the eastern flank of the volcano in general, however one normal faulting mechanism was also calculated (Figure 7, #6). The focal mechanisms for each of the fault plane solutions are

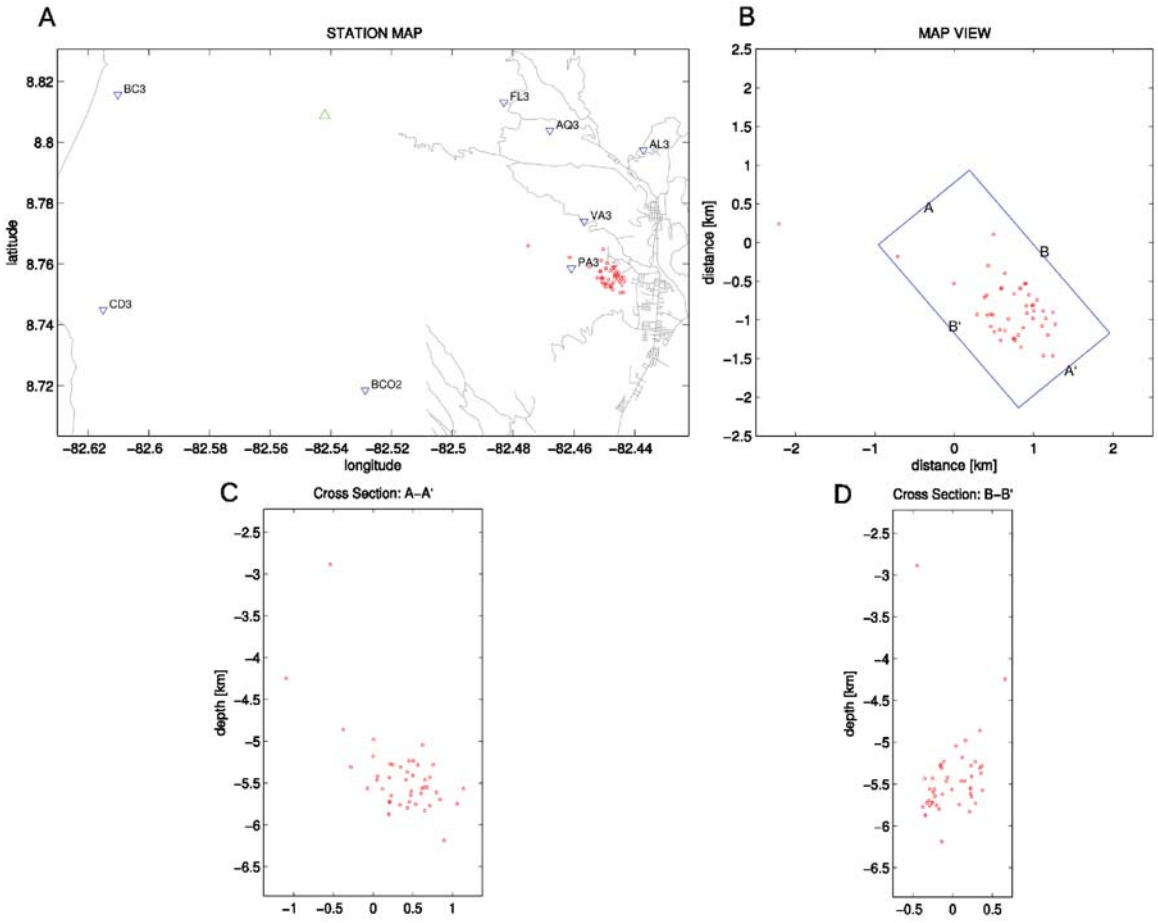

Figure 6: Figure showing final hypocenters calculated using HypoDD. Grey lines in Fig. 6A represent roads, blue inverted triangles represent stations and the single green triangle symbolizes the summit of Barú. 6B shows the cluster in greater detail as well as the dimensions of the depth cross sections shown in 6C and 6D.

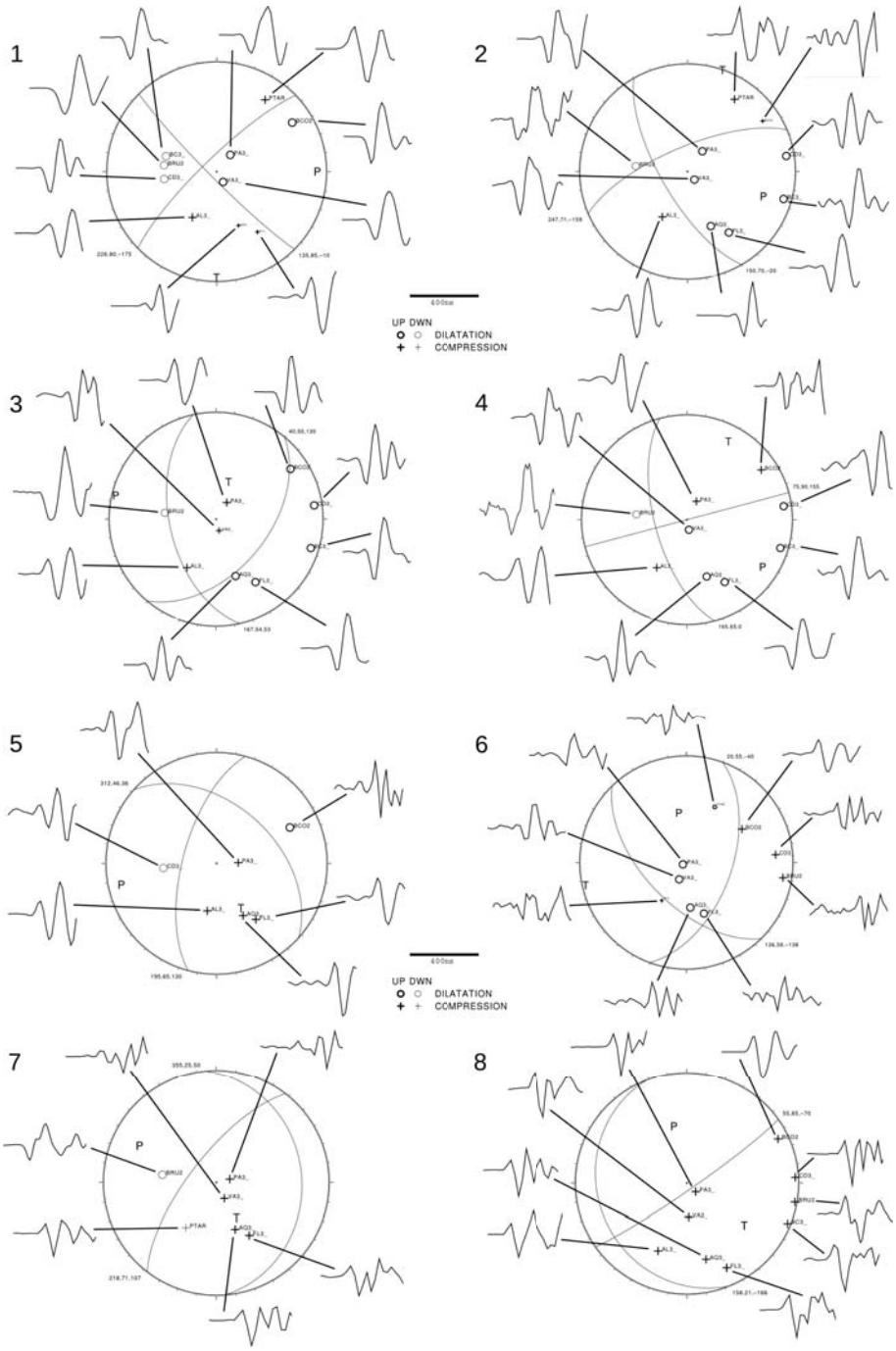

Figure 7: Focal mechanisms for 8 events and accompanying waveforms. Circles signify downward first motions whereas plus signs signify upward motions. The size of the symbol denotes the weighting of the pick (small symbols indicate lower weighting). These focal mechanisms are plotted in map view in Figure 9 and are numbered accordingly. Plots generated using FPFIT *and* FPPLOT (Reasenberg and Oppenheimer, 1985).

also plotted in Figure 9 and numbered 1-8, corresponding to the numbers in Figure 7. Polarity picks for certain waveforms were downweighted when the first motion was slightly ambiguous. Often this was due to a station being located near a nodal plane which led to weak first motions on the seismogram. In most cases, however, changing of these unweighted picks from up to down or vice-versa would have a small effect on the overall solution. Focal mechanisms for the majority of the Volcancito cluster are unattainable given low signal to noise ratios but these results appear to agree with previous results which indicated largely strike-slip and reverse faulting in the area (Camacho et al., 2008; Camacho, 2009; Toral and Ho, 2006).

Figure 8 shows focal mechanisms for the region surrounding the Panama Triple Junction from the Global CMT database (www.globalcmt.org). The direction of maximum compressional stress for the region is roughly NNE-SSW which is accommodated on right-lateral transverse faults in the area of the PFZ and BFZ, transitioning to reverse faulting towards Punta Burrica and southern Costa Rica. These data are in contrast to the results presented here as well as previous studies of the area around Volcán Barú which show predominantly E-W or NW-SE principal stress axes (Figure 9). LaFemina and others (2009) have postulated that an E-W component of forearc motion in southern Costa Rica may be explained as a form of tectonic escape from the subducting, relatively rigid Cocos Ridge. If this is the case, E-W to NW-SE trending principal stresses near Barú may reflect forearc motion eastward along the trench.

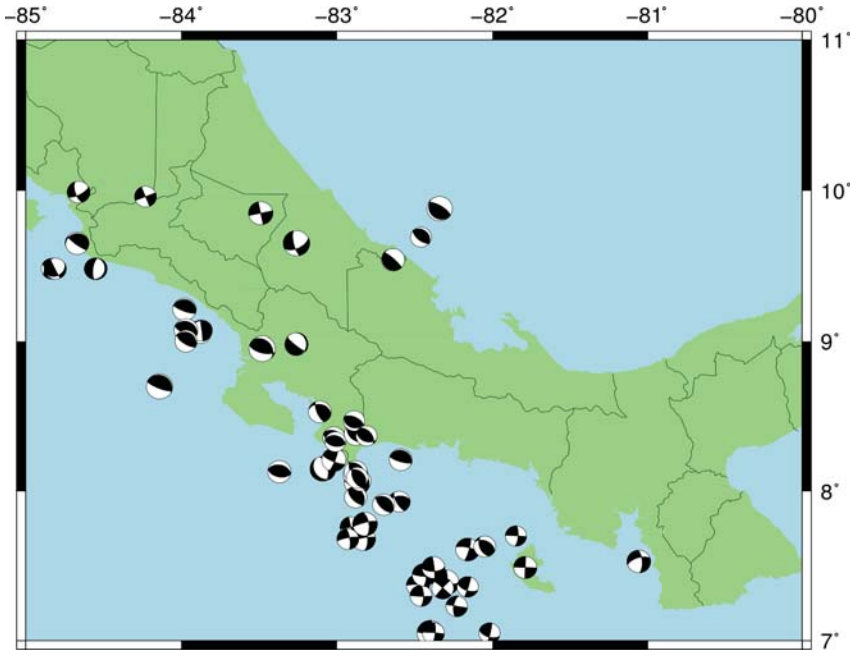

Figure 8: Regional focal mechanisms for all events at 0-15 km depth for the area surrounding the Panama Triple Junction . Data from 1975 through June 2015. Source: www.globalcmt.org

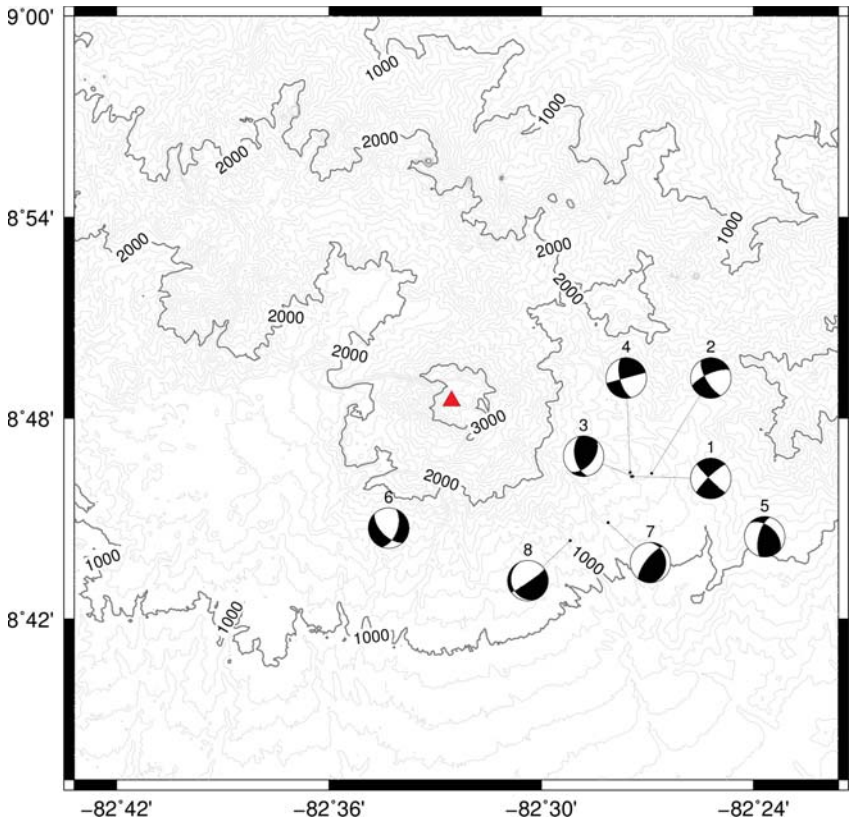

Figure 9: Focal mechanisms for the area around Volcán Barú. The red triangle marks the summit of Barú. Contours are in meters.

Tables 1A and 1B summarize event magnitudes for the Barú catalog. Table 1A includes 36 events which were initially detected via the STA/LTA detection method but excludes those events of the initial 91 which lie well outside the network. Highlighted in grey are the template events used for the template matching detection technique. Table 1B includes all of the events detected by template matching but does not include their location as they were considered to have the same source for the purposes of duration magnitude calculation after Lee and others (1972). Given the small differences in hypocenter location amongst the cluster (Figure 6) and the small weight given to event-station distance in the duration magnitude calculation, considering each event to have the same source location should have a very small effect on the magnitudes calculated.

Magnitudes for the entire catalog range from 0.04 to 3.18 M_d. As would be expected, events in Table 1B are of smaller magnitude (0.04-1.17 M_d) than events in Table 1A as they were only detected once the template matching technique had been applied.

Conclusions

A new, year-long seismic catalog for Volcán Barú was presented in this study

using data from a temporary, 10-station network. Ninety-one local events were detected and used to calculate a 1-D velocity model for Barú. In relocating these 91 events using the newly calculated velocity model, a small cluster of seven events was identified. A template matching technique similar to that implemented by Shelly and others (2007) used these seven events as templates to further investigate the cluster. An additional 47 smaller magnitude events were detected using this technique. All events from the cluster were then relocated using double difference relocation methods. Waveforms, a spectrogram, focal mechanisms and duration magnitudes are presented as part of the

Table 1: Table showing signal duration magnitudes for events detected by both the Antelope STA/LTA algorithm (Table 1A) and template matching technique (Table 1B).

Table 1A

Date	Time	Lat	Long	Depth (km)	M_d
5/30/2013	11:56:22.315	8.767	-82.3986	14.0812	1.65
6/03/2013	9:27:46.585	8.7537	-82.4359	18.1561	2.18
6/03/2013	22:07:26.939	8.7804	-82.4437	7.6939	1.86
6/22/2013	10:08:41.482	8.7349	-82.46	16.8018	2.14
6/27/2013	10:07:57.808	8.7155	-82.4396	16.48	1.65
7/05/2013	7:30:24.814	8.7992	-82.4253	14.3057	1.50
7/17/2013	10:21:08.145	8.8305	-82.4634	5.5708	1.29
7/20/2013	4:49:50.492	8.6871	-82.5078	9.9689	3.18
8/19/2013	2:49:48.166	8.7637	-82.4739	8.2172	1.02
9/04/2013	18:33:21.414	8.8239	-82.467	3.9011	0.97
9/07/2013	13:37:26.947	8.6833	-82.4046	11.769	1.24
10/11/2013	16:11:23.263	8.775	-82.4365	5.229	2.17
10/11/2013	16:19:21.285	8.7504	-82.4201	1.8104	0.87
10/11/2013	16:47:43.804	8.7758	-82.4363	5.0601	1.76
10/11/2013	17:13:45.904	8.7743	-82.4214	5.0702	1.18
10/17/2013	2:45:31.464	8.7481	-82.448	1.4833	0.83
10/29/2013	6:10:22.975	8.7228	-82.5717	25.0882	1.06
12/05/2013	18:07:09.514	8.7621	-82.4355	3.478	0.93
12/08/2013	17:24:57.677	8.7678	-82.4346	5.4215	1.39
12/10/2013	3:54:22.282	8.7662	-82.4301	5.6191	2.09
12/10/2013	4:08:09.293	8.7679	-82.4313	5.524	0.83
12/14/2013	11:18:30.775	8.7168	-82.4688	19.8918	1.43
12/21/2013	8:30:04.574	8.7677	-82.4377	8.4828	1.12
12/25/2013	5:23:55.333	8.7142	-82.4721	20.231	1.39
1/17/2014	16:25:28.009	8.7867	-82.6495	0	1.68
1/21/2014	10:14:53.151	8.6264	-82.5214	17.4091	1.33
1/23/2014	2:17:10.995	8.7729	-82.3926	6.6325	1.53
1/29/2014	5:07:49.974	8.7403	-82.6412	37.7917	1.84
1/31/2014	15:22:43.437	8.7741	-82.4551	0	0.95
2/02/2014	10:58:36.602	8.7093	-82.4594	18.6631	1.56
2/10/2014	11:07:09.587	8.7822	-82.4118	0	1.25
3/13/2014	22:47:24.019	8.7564	-82.6719	24.1721	1.70
3/22/2014	0:30:59.406	8.7318	-82.4682	13.8966	1.15
3/27/2014	11:00:32.476	8.738	-82.4004	15.2373	1.17
3/29/2014	5:33:06.084	8.7818	-82.6416	0	1.87
4/11/2014	1:01:49.601	8.8075	-82.6505	0	2.23

Table 1B

Date	Time	M_d
01/03/14	03:45:49.20	0.28
02/05/14	23:50:25.48	0.31
01/06/14	18:35:59.00	0.54
01/07/14	00:49:26.60	0.61
01/11/14	02:50:15.52	0.39
01/11/14	04:37:36.56	0.34
01/16/14	17:27:47.12	0.50
01/25/14	07:12:13.80	0.57
02/10/14	13:17:23.24	0.68
02/14/14	17:30:30.52	0.61
03/21/14	02:47:26.84	0.61
03/21/14	11:12:59.68	1.08
10/11/13	16:13:30.64	0.31
10/11/13	16:16:52.76	0.69
10/11/13	16:19:19.96	1.17
10/11/13	16:36:31.40	0.94
10/11/13	16:49:06.00	0.16
10/11/13	17:01:00.48	0.73
10/11/13	17:13:45.00	0.87
10/11/13	17:47:55.80	0.49
10/11/13	18:12:07.92	0.74
10/11/13	18:45:06.96	0.82
10/11/13	19:39:01.08	0.30
10/11/13	20:17:37.20	0.64
10/12/13	07:57:22.72	0.12
10/12/13	13:28:25.40	0.38
10/13/13	11:45:49.68	0.38
10/16/13	06:34:38.04	0.95
10/16/13	06:36:34.24	0.16
10/16/13	16:18:23.80	0.71
10/17/13	02:45:29.64	0.97
10/17/13	15:36:06.24	0.55
10/21/13	15:36:07.76	0.39
10/23/13	07:04:00.96	0.46
10/30/13	18:49:32.80	0.35
11/03/13	13:37:48.28	0.89
11/11/13	15:46:20.72	0.04
11/11/13	15:48:59.96	0.16
11/17/13	13:15:57.00	0.82
12/08/13	22:46:27.52	0.16
12/10/13	03:57:25.08	0.36
12/10/13	04:00:33.96	0.25
12/10/13	05:05:55.28	0.24
12/10/13	05:43:55.16	0.20
12/27/13	20:43:48.16	0.46
12/27/13	22:15:02.68	0.16
12/28/13	01:11:13.96	0.14

catalog.

These earthquakes have large frequency bands suggesting largely tectonic processes are responsible for these events, although the role of volcanic processes in local seismicity is not ruled out. The focal mechanisms calculated suggest that the predominant mechanisms in this area may be strike-slip and reverse faulting although more well-recorded events are needed to confirm whether or not a larger variety of mechanisms are present. These results are in agreement with past work by Camacho (et al., 2008; 2009), Toral and Ho (2006) and Cowan et al. (1996) which concluded that local faulting was predominantly strike-slip or reverse in nature. Principal stress axes oriented E-W and NW-SE are in contrast with regional stresses which trend roughly N-S. This may reflect trench-parallel forearc movement (LaFemina et al., 2009).

Works Cited

Adamek, S., Frohlich, C., & Pennington, W. D. (1988). Seismicity of the Caribbean-Nazca boundary: Constraints on microplate tectonics of the Panama region. *Journal of Geophysical Research: Solid Earth (1978–2012)*, *93*(B3), 2053-2075.

Astigarrabia, E. C. (2003). SISMOTECTÓNICA DEL EXTREMO NORTE DE LA ZONA DE FRACTURA DE PANAMÁ. *Tecnoniencia, 5(2), 139-151*.

Camacho, E., & Víquez, V. (1993). Historical seismicity of the north Panama deformed belt. *Revista Geológica de América Central*, (15).

Camacho, E., Novelo-Casanova, D. A., Tapia, A., & Rodriguez, A. (2008, December). Seismicity at Baru Volcano, Western Panama, Panama. In *AGU Fall Meeting Abstracts* (Vol. 1, p. 2051).

Camacho, E. C. (2009). SISMICIDAD DE LAS TIERRAS ALTAS DE CHIRIQUÍ. *Tecnociencia, 11(1), 119-130.*

Camacho, E., Hutton, W., & Pacheco, J. F. (2010). A new look at evidence for a Wadati–Benioff zone and active convergence at the north Panama deformed belt. *Bulletin of the Seismological Society of America*, *100*(1), 343-348.

Carr, M. J., Feigenson, M. D., Patino, L. C., & Walker, J. A. (2003). Volcanism and geochemistry in Central America: Progress and problems. *Inside the subduction factory*, 153-174.

Cowan, H.A., Sánchez L., Camacho E., Palacios J., Tapia A., Irving D., Esquivel D. & Lindholm C. (1996). Seismicity and tectonics of Western Panama from new portable seismic array data, *Final Report to the Research Council of Norway*, NTNF-NORSAR, Kjeller, Norway. 23pp.

Cowan, H. A., Machette, M. N., Haller, K., & Dart, R. (1998). Map and database of Quaternary faults and folds in Panamá and Its offshore Regions. *International Lithosphere Program, Task Group II-2, Major Active Faults of the World, USGS. Open File*, 98-779.

de Boer, J. Z., Defant, M. J., Stewart, R. H., & Bellon, H. (1991). Evidence for active subduction below western Panama. *Geology*, *19*(6), 649-652.

Defant, M. J., Clark, L. F., Stewart, R. H., Drummond, M. S., de Boer, J. Z., Maury, R. C., ... & Restrepo, J. F. (1991). Andesite and dacite genesis via contrasting processes: the geology and geochemistry of El Valle Volcano, Panama. *Contributions to Mineralogy and Petrology*, *106*(3), 309-324.

Defant, M. J., Jackson, T. E., Drummond, M. S., De Boer, J. Z., Bellon, H., Feigenson, M. D., ... & Stewart, R. H. (1992). The geochemistry of young volcanism throughout western Panama and southeastern Costa Rica: an overview. *Journal of the Geological Society*, *149*(4), 569-579.

Herrick, J. A., Siebert, L., & Rose, W. I. (2013). Large-volume Barriles and Caisán debris avalanche deposits from Volcán Barú, Panama. *Geological Society of America Special Papers*, *498*, 141-162.

Hidalgo, P. J., & Rooney, T. O. (2010). Crystal fractionation processes at Baru volcano from the deep to shallow crust. *Geochemistry, Geophysics, Geosystems*, *11*(12).

Hidalgo, P. J., & Rooney, T. O. (2014). Petrogenesis of a voluminous Quaternary adakitic volcano: the case of Baru volcano. *Contributions to Mineralogy and Petrology*, *168*(3), 1-19.

Kissling, E., Ellsworth, W. L., Eberhart-Phillips, D., & Kradolfer, U. (1994). Initial reference models in local earthquake tomography. *Journal of Geophysical Research: Solid Earth (1978–2012)*, *99*(B10), 19635-19646.

LaFemina, P., Dixon, T. H., Govers, R., Norabuena, E., Turner, H., Saballos, A., ... & Strauch, W. (2009). Fore-arc motion and Cocos Ridge collision in Central America. *Geochemistry, Geophysics, Geosystems*, *10*(5).

Lee, W. H. K., Bennett, R. E., & Meagher, K. L. (1972). *A method of estimating magnitude of local earthquakes from signal duration* (pp. 1-28). US Department of the Interior, Geological Survey.

Morell, K. D., Gardner, T. W., Fisher, D. M., Idleman, B. D., & Zellner, H. M. (2013). Active thrusting, landscape evolution, and late Pleistocene sector collapse of Barú Volcano above the Cocos-Nazca slab tear, southern Central America. *Geological Society of America Bulletin*, *125*(7-8), 1301-1318.

Muñoz, A. V. (1988a). Seismicity of the Panama Block I. Magnitudes and spatial distribution of epicentres. *Tectonophysics*, *145*(3), 213-224.

Muñoz, A. V. (1988b). Tectonic patterns of the Panama Block deduced from seismicity, gravitational data and earthquake mechanisms: Implications to the seismic hazard. *Tectonophysics*, *154*(3), 253-267.

Reasenberg, P., & Oppenheimer, D. H. (1985). *FPFIT, FPPLOT and FPPAGE; Fortran computer programs for calculating and displaying earthquake fault-plane solutions* (No. 85-739). US Geological Survey,.

Restrepo, J. F. (1987). *A geochemical investigation of Pleistocene to recent calc-alkaline volcanism in western Panama: Tampa, University of South Florida* (Doctoral dissertation, master's thesis).

Shelly, D. R., Beroza, G. C., & Ide, S. (2007). Non-volcanic tremor and low-frequency earthquake swarms. *Nature*, *446*(7133), 305-307.

Sherrod, D. R., Vallance, J. W., Espinosa, A. T., & McGeehin, J. P. (2007). Volcán Barú—Eruptive History and Volcano-Hazards Assessment. *US Geological Survey Open-File Report*, *2007*, 1401.

Timing. (n.d.). Retrieved May 25, 2015, from http://www.osop.com.pa/sixaola-sphinx-doc/_build/html/timing.html#timing

Toral Boutet, J., & Ho G., C. A. Monitoreo Y Análisis Preliminar De La Sismicidad Alrededor De Boquete: Mayo 04-10, 2006. *Web. 16 Feb. 2015.* <http://www.cei.utp.ac.pa/documentos/2010/pdf/InfoBolquete2.pdf>.

UTP, 1992, Evaluación de la amenaza, estimación de la vulnerabilidad y del factor costo del riesgo del Volcán Barú, Republica de Panamá: Panama, *Departamento de Geotécnica Facultad de Ingenieria Civil, Universidad Tecnológica de Panamá*, p. 129.

Waldhauser, F., & Ellsworth, W. L. (2000). A double-difference earthquake location algorithm: Method and application to the northern Hayward fault, California. *Bulletin of the Seismological Society of America*, *90*(6), 1353-1368.

Wegner, W., Wörner, G., Harmon, R. S., & Jicha, B. R. (2011). Magmatic history and evolution of the Central American Land Bridge in Panama since Cretaceous times. *Geological Society of America Bulletin*, *123*(3-4), 703-724.

Appendix A

Prompted by the May 2006 swarm, the first local monitoring effort at Barú was undertaken by Toral and Ho (2006). A team from the Universidad Tecnológica de Panamá installed a temporary network two days after the onset of the swarm. It is important to note that events occurring before the installation of the temporary network (May 8th) were located using only the arrivals at two stations in the city of David (~40km distant) and therefore should be subject to skepticism (See Figure 10).

Also following the 2006 swarm, the University of Panama in conjunction with the Panamanian government and with the help of OSOP began to install a permanent seismic monitoring network on Barú. Shown in Figure 11 are all of the local events in the UPA catalog from January 2006 through December 2008, most of which occurred in May 2006 during and following the swarm. It is important to note that these events were not all detected while each of these stations was operational. More likely, stations were installed one-by-one over time. Note that the level of seismicity east of the summit is much greater than west of the volcano which agrees with the findings of this study.

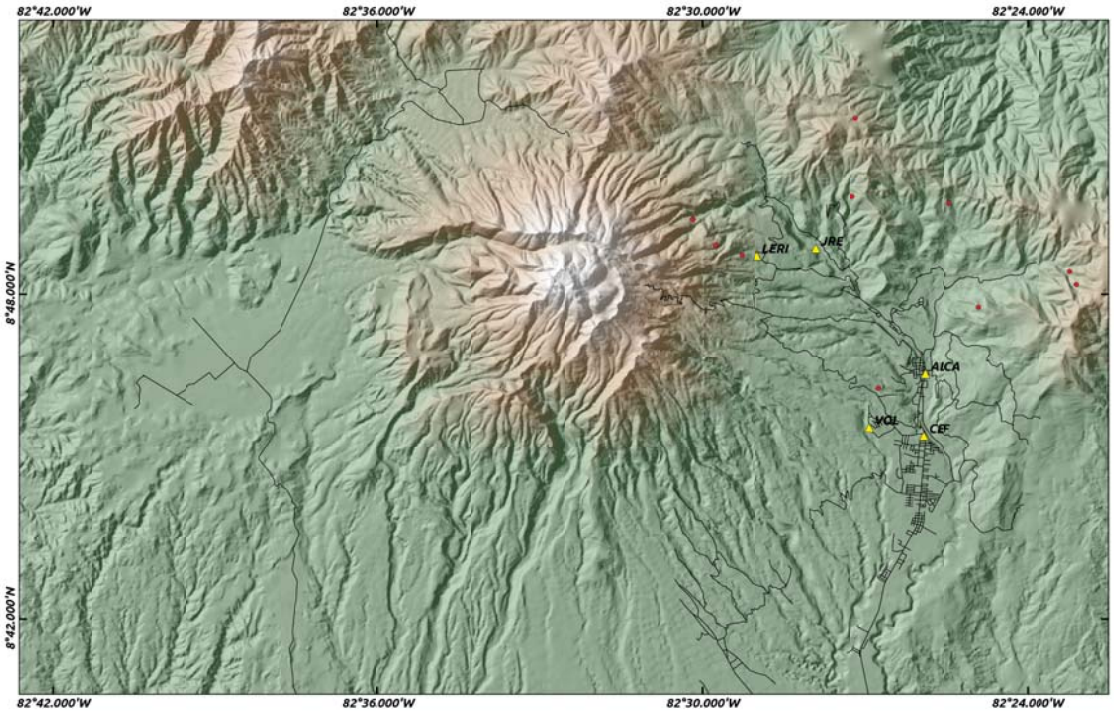

Figure 10: Map showing the locations of the temporary network installed by Toral and Ho during the 2006 swarm (yellow triangles). Red dots symbolize the locations of the earthquakes recorded both before and after installation of this network.

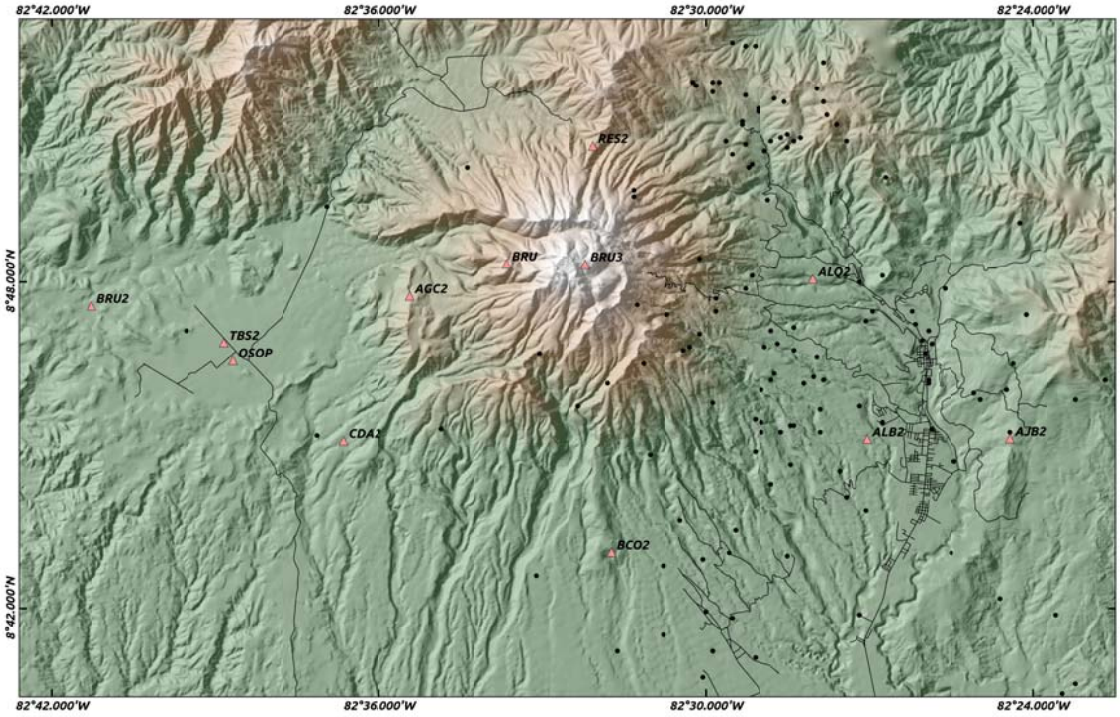

Figure 11: Station locations for the UPA network 2006-2008 (pink triangles). Earthquakes recorded on this network from 2006-2008 are marked by black dots.

Appendix B

Table 2: Station information for the sites used in this study. Yellow fields indicate stations that are still operated by the University of Panama. Station BRU2 (blue) is operated by OSOP. Green stations were installed by the author and were removed at the end of this project.

Station ID	Location	Lat	Long	Elevation (m)	Sensor	Components
VBFL3	Finca Lerida	8.81305	-82.48302	1692	Darien	Vertical
VBAQ3	Alto Quiel	8.80379	-82.46780	1505	Darien	Vertical
VBAL3	Alto Lino	8.79745	-82.43719	1240	Darien	Vertical
VBVA3	Volcancito Arriba	8.77402	-82.45666	1413	Darien	Vertical
VBPA3	Palmira Arriba	8.75860	-82.46084	1280	Darien	Vertical
VBBC3	Paso Ancho	8.81559	-82.61026	1675	Darien	Vertical
VBCD3	Cordillera	8.74488	-82.61514	1335	Darien	Verical
BRU2	Barriles	8.79400	-82.68783	1308	Trillium Compact	Triaxial
BCO2	Cerro Banco	8.71850	-82.52867	1429	Sixaola	Triaxial
PTAR3	Potrerillos Arriba	8.69280	-82.49610	982	Darien	Vertical